Advances in Engineering Software 42 (2011) 76–84

Contents lists available at ScienceDirect

Advances in Engineering Software

journal homepage: www.elsevier.com/locate/advengsoft

Force-torque based on-line tool wear estimation system for CNC milling of Inconel 718 using neural networks

Bulent Kaya [a,*], Cuneyt Oysu [b], Huseyin M. Ertunc [b]

[a] Erciyes University, Kayseri Vocational High School, 38020 Kayseri, Turkey
[b] Kocaeli University, Mechatronics Engineering Department, Kocaeli, Turkey

ARTICLE INFO

Article history:
Received 2 May 2008
Received in revised form 23 April 2010
Accepted 13 December 2010
Available online 13 January 2011

Keywords:
On-line monitoring
Cutting forces
Torque
Wear
Milling
Neural networks

ABSTRACT

In a modern machining system, tool condition monitoring systems are needed to get higher quality production and to prevent the downtime of machine tools due to catastrophic tool failures. Also, in precision machining processes surface quality of the manufactured part can be related to the conditions of the cutting tools. This increases industrial interest for in-process tool condition monitoring (TCM) systems. TCM supported modern unmanned manufacturing process is an integrated system composed of sensors, signal processing interface and intelligent decision making strategies. This study includes key considerations for development of an online TCM system for milling of Inconel 718 superalloy. An effective and efficient strategy based on artificial neural networks (ANN) is presented to estimate tool flank wear. ANN based decision making model was trained by using real time acquired three axis (F_x, F_y, F_z) cutting force and torque (M_z) signals and also with cutting conditions and time. The presented ANN model demonstrated a very good statistical performance with a high correlation and extremely low error ratio between the actual and predicted values of flank wear.

1. Introduction

Tool wear is an important factor which affects the machined surface characteristics. During the manufacturing processes, machined part surfaces get more or less destroyed depending on the cutting forces caused by worn tools. Larger cutting forces generate poor surface finish as well as extensive surface damage [1]. This destruction is decisive for the later characteristics of the manufactured part such as sliding, lubricating, corrosion resistance, contact, fatigue, fracture and straightness properties. Tool wear estimation is therefore not only a diagnostics requirement to prevent machine-tool failure and production-material waste, but also plays crucial role which mainly affects the dimensional integrity, better performance and service-life of machined components.

Unfortunately, there is no direct way to measure tool wear without interrupting the machining process. CNC operators usually decide the tool wear level off-line via visual inspection of cutting edges or on-line with sound level related to their experience. Today's modern unmanned CNC manufacturing machines require robust on-line tool condition monitoring systems. In-process tool condition monitoring (TCM) system is an approach to indirectly detect the tool wear level in machining. High sensitive sensor equipments integrated to machine tools together with an efficient mathematical model are necessary for a robust on-line tool wear monitoring system.

A general TCM system development stage is divided into four main phases; (1) the planning phase (design of experiment), (2) application phase, (3) data acquisition and signal processing phase, and (4) analysis phase. For the planning and application phase, utilization of different sensors has been reported in on-line TCM research area such as, dynamometer, accelerometer, motor load current, acoustics emission, temperature, optical and sensor fusion techniques. However, most of these on-line TCM techniques have been conducted on lathes which use non-rotating single tools [2–16]. In milling however, tool wear progression is different as the cutting edge enters and exits the workpiece repeatedly throughout the process. In addition, rotating motion of milling cutters makes it difficult to attach the sensors close to the cutter-work-piece interface [17]. TCM systems, developed for turning processes, are therefore not guaranteed to work satisfactorily for a semi-intermitted process like grinding or a fully intermitted process like milling [18]. Recently some researchers have developed TCM systems using various sensors and different wear estimation techniques for milling. Ghosh et al. [18] used cutting forces, spindle vibration, spindle current, and sound pressure level for ANN based flank wear estimation. Iqbal et al. developed an in-process fuzzy expert flank wear monitoring system based on measured peak values of two components of force signals (F_x and F_y) using a dynamometer [19]. Tseng and Chou proposed a rule based tool

* Corresponding author. Tel.: +90 352 437 49 15.
E-mail address: bulentkaya@erciyes.edu.tr (B. Kaya).

0965-9978/$ - see front matter © 2010 Elsevier Ltd. All rights reserved.
doi:10.1016/j.advengsoft.2010.12.002

monitoring system for end milling, based on spindle motor current [20].

The objective of this work is to develop a robust TCM system for end milling of Inconel 718. Inconel 718, as a difficult-to-cut superalloy, is widely used in aerospace and gas turbine industries. It is especially used in aircraft engine parts, high-speed airframe parts such as wheels, valves, buckets, spacers, and high temperature bolts and fasteners in severe operation conditions. With such a robust on-line tool condition monitoring system, especially companies that have long production runs with difficult-to-cut superalloys such as Inconel 718 on their machining centers, an efficient tool maintenance (changing inserts or worn tools) can be accomplished. Since the sudden failure of the worn cutting tool deteriorates the machining surface, it is possible to obtain a certain surface quality with an accurate prediction of tool wear.

The current paper presents evaluation of cutting conditions on tool life and proposes an effective hybrid strategy to estimate tool flank wear while milling of Inconel 718 superalloy. In this proposed strategy, three axis cutting force, torque, cutting conditions and cutting time data are combined with measured tool flank wear data to create an Artificial Neural Network (ANN) model. The ANN model is then verified with measured data. Using this ANN model, an online tool tracking system is developed for monitoring the flank wear of the main cutting edge. The system indicates whether tools are performing efficiently or are not.

2. Experimental setup

2.1. Taguchi based orthogonal array experimental design

Taguchi's orthogonal array structure offers robust experimental design with decreased experiment number. Taguchi method involves analysis between the factors, their interactions and responses. The method is widely used in engineering applications. Taguchi's orthogonal array structure was used for experimental design, as reduced number of experiments can be acceptable for industry. A standard Taguchi orthogonal array L9 (3^3) was chosen for the most controlled factors such as, cutting speed (Vc), Feed per tooth (Sz) and Depth of cut (Doc). Radial depth of cut factor was kept at a constant value of 1 mm during the experiments because material removal rate can be controlled with depth of cut factor. Three levels of milling process factors were selected according to tool manufacturer's recommendations as given in Table 1.

2.2. Work material and cutting tool

In this study, superalloy Inconel 718 was used for experiments. Several studies have been done by the researchers for investigating the effects of changing operating parameters on the tool life, productivity and tool wear patterns obtained when machining of Inconel 718 [21–26]. Table 2 shows the chemical composition of Inconel 718 having an average hardness of 40 Rc used in this experiment. The material was initially machined for a rectangular block shape of 70 × 62 × 70 mm. Sandvik inserts (R390-11 T3 08M-PL 1030) mounted on (R390-016A16-11L) cutter body with 16 mm diameter was chosen for experimental cuts at dry cutting conditions.

Table 1
Three level Taguchi Design, Factors and levels.

Factors and their levels Factors	Levels		
	1	2	3
V_c, cutting speed (m/min)	50	75	100
S_z, feed per tooth (mm/tooth)	0.06	0.09	0.12
Doc, depth of cut (mm)	0.3	0.45	0.6

2.3. Milling experiments and measuring instruments

The milling tests were conducted on five axis rotary table type Deckel-Maho DMU 60P CNC machining center. Planar and down-milling type CAM strategy was generated by using ProEngineer Wildfire PLM software to automate each experiment. The rotating cutting force dynamometer (Kistler Corporation, Model 9123C1111) is used for the dynamic and quasistatic measurement of the three force components (F_x, F_y, F_z) as well as of the drive moment M_z on a rotating tool. The rotating cutting force type dynamometer (RCD) has advantages over fixed dynamometers, such as the cutting forces can be measured on the rotating tool independently of the size of workpiece and measurement can be performed on any spatial position (four or five axis milling). The cutter body was mounted with a single insert on RCD. The tool cutting edge is aligned with RCD's zero count groove on the principal *Y* axis of the RCD dynamometer. The output from the cutting dynamometer is transferred with a non-contact Radio Frequency protocol to charge amplifier (Kistler Corporation, Model 5223B). Fig. 1 shows the machine tool, workpiece and RCD setup for experimental study.

3. Experimental results

Nine experiments have been carried out at different cutting conditions according to Taguchie's orthogonal array design as given in Table 3.

Three cutting force components (F_x, F_y, F_z) on principle axis directions and torque data were collected differentially using NI 6229 multifunction PCI data acquisition card together with NI BNC 2110 connection block. Required data acquisition software was written by using MATLAB DAQ toolbox v2.9 [27] and data acquired with 15 KSample/s sampling rate. The cutting process was interrupted at different time intervals depending on the performed cutting condition and wear propagation. There are several types of tool wear damages observed at the tool tip during the experiments. Crater, chipping, notching and flank wear are the observed wear mechanisms. Generally the end of tool life is determined by the excessive wear at the tool flank face. Maximum wear length at the flank face of the tool was measured as wear land by using Nikon Eclipse L150 microscope at 50× magnification and ImageJ software [28] according to ISO 8688-2 throughout the whole of the machining tests. The measurement of flank wear for a sample is shown in Fig. 2. The maximum flank wear criteria for each insert were assigned to be approximately 500 μm.

Collected signals shown in Fig. 3 have to be processed in order to develop an online TCM system. The cutting force and torque signals acquired after each interrupting cut was processed with RMS, which is the most common statistical feature extraction method as:

$$(F_x, F_y, F_z, M_z)_{rms} = \sqrt{\frac{1}{n}\sum_{i=1}^{n}(F_x, F_y, F_z, M_z)(i)^2} \quad (1)$$

Table 2
Chemical composition of Inconel 718 (wt.%).

Ni	Cr	Cb + Ta	Mo	Ti	Al	Co	Si	Mn	C	Fe
53.8	18.2	5.26	2.96	0.94	0.44	0.3	0.09	0.064	0.028	Balanced

Fig. 1. Experimental setup – machine tool, close-up view of workpiece and RCD setup.

Table 3
List of cutting conditions performed.

Experiment no.	Doc (mm)	Vc (m/min)	Sz (mm/rev)
1	0.6	100	0.12
2	0.6	75	0.09
3	0.6	50	0.06
4	0.45	100	0.09
5	0.45	75	0.06
6	0.45	50	0.12
7	0.3	100	0.06
8	0.3	75	0.12
9	0.3	50	0.09

where n represents the total number of data in each cut as indicated in Fig. 3. For identification of online TCM system overall 170 wear stages were measured in nine different experiments.

Nine experiments have been carried out at different cutting conditions according to Taguchie's orthogonal array design, as given in Table 1. Fig. 4 shows, tool flank wear (V_B) measurements plotted against time for each of nine experiments.

All the graphs shown in Fig. 4a–i indicate a gradual increase of the flank wear with progressive time. In general, low (0.3 mm) and medium level (0.45 mm) of depth of cut (Doc) values generates strong linear trend between cutting time and gradually increased tool flank wear. Results show that the development of the flank tool wear was relatively rapid in the level of 0.6 mm depth of cut.

The main effects of Signal to Noise ratio (SNR) for the tool life are shown in Fig. 5. Maximum level of cutting speeds and depth of cut (Doc) give faster removal rates but also produce fast excessive edge cratering and flank wear. The minimum tool life for the maximum values of the cutting conditions shown in Fig. 4a is 5.76 min. Fig. 5 shows that minimum level of cutting conditions (Vc = 50 m/min, Sz = 0.06 mm/rev, Doc = 0.3 mm) will give the maximum tool life according to Taguchi analysis.

Analysis of variance (ANOVA) for tool life represents the evaluation of the effects of cutting conditions as given in Table 3. In Table 4, P-values test the statistical significance of each of the factors. Since none of the P-values are less than 0.1, the factors have no statistically significant effect on tool life even at the 90.0% confidence level. However, it is observed from the ANOVA table that depth of cut and cutting speed have more influence on the tool life than feed rate.

Figs. 6–8ac show various graphs of tool flank wear plotted against cutting forces and torque for depth of cuts of 0.6–0.45 mm and 0.3 mm at different cutting conditions respectively.

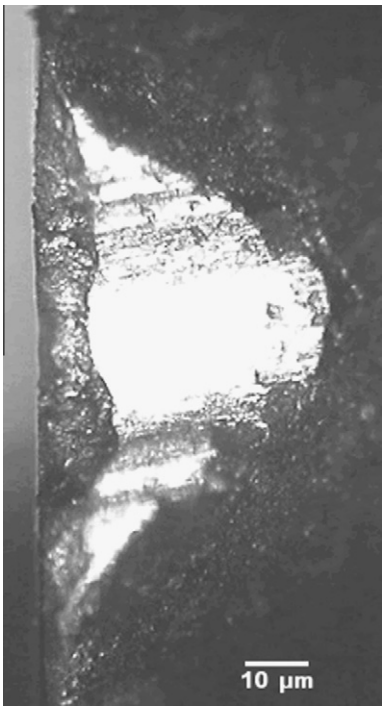

Fig. 2. Sample wear measurement at conditions of experiment 7.

Figs. 6–8 show that, cutting forces and torque have an upward trend while tool wear increases. The cutting forces, particularly the axial cutting force component F_z and the torque (M_z), decreased gradually as shown in Fig. 6a–c, as the flank wear progressed. This is for another wear mechanism, the crater wear, which affects the cutting forces and torque. Growths in crater wear causes cutting forces and torque to decrease. The reason for this is the increase in effective rake angle 16 due to the crater wear. It was observed however that, this decreasing trend of the cutting forces and torque was not long. For a larger form of the crater and flank wear, effective rake angle decreased 16. As a result cutting forces and torque increased again to previous levels with rapid tool wear propagation.

Torque (M_z) and F_z components of RCD dynamometer signals are more sensitive to tool flank wear as compared with F_x and F_y

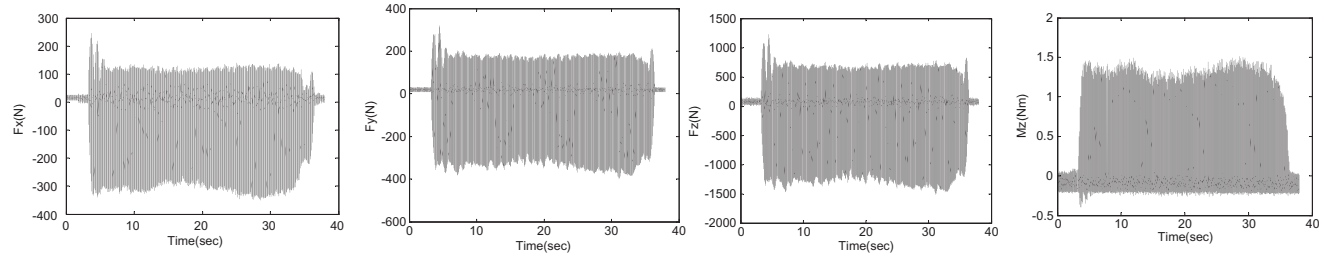

Fig. 3. Sample plot of acquired cutting forces (F_x, F_y, F_z) and torque (M_z) (corresponding wear case shown in Fig. 2).

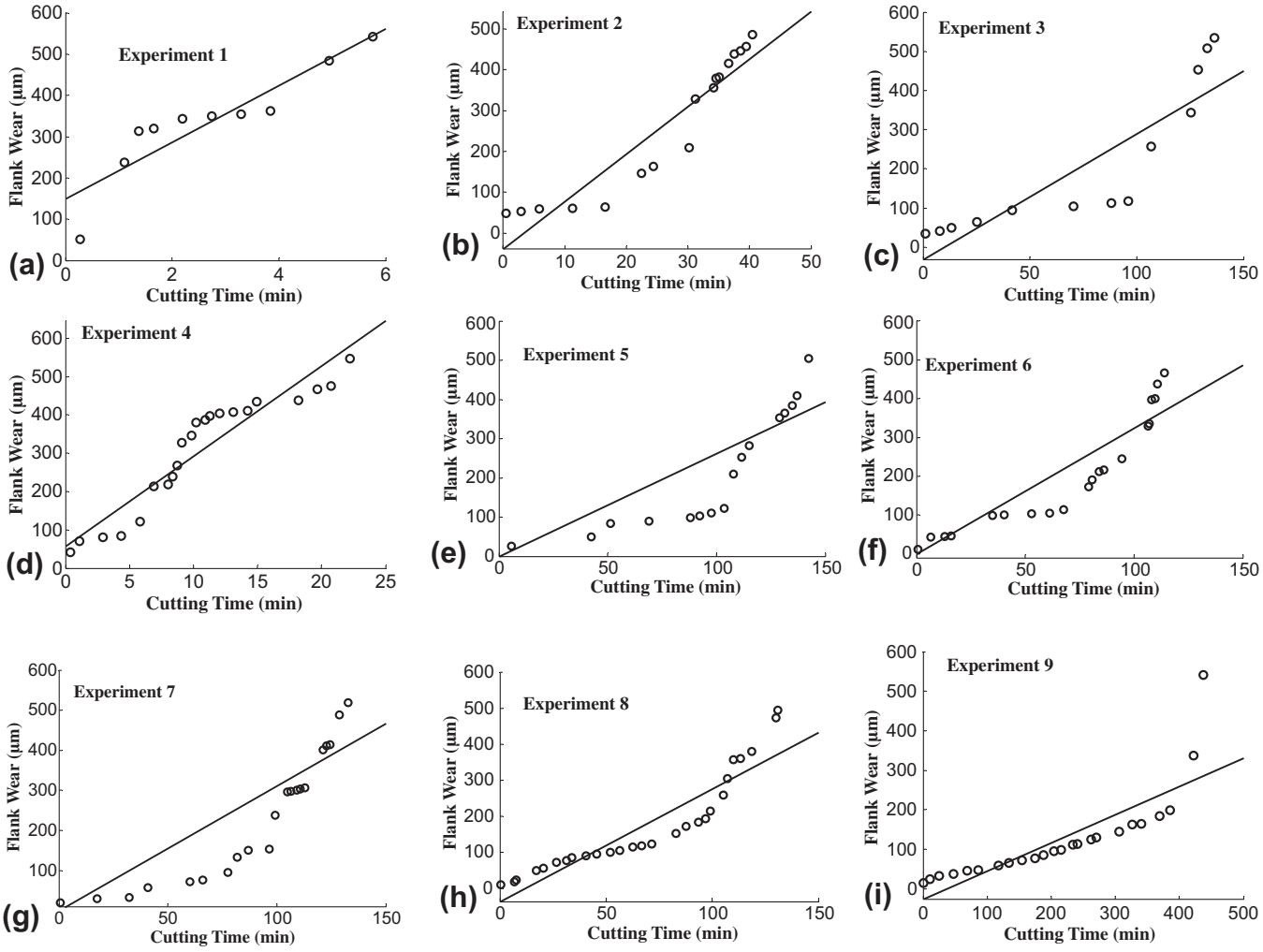

Fig. 4. Tool life versus time, according to nine experiments.

signals as indicated in Figs. 6a–c to 8a–c. However it is difficult to decide which signals is actually more important on estimating tool wear. Therefore, for analyzing influence of tool flank wear propagation on cutting forces (F_x, F_y, F_z) and torque (M_z) linear regression analysis was completed on the data plotted in Figs. 6a–c to 8a–c.

Multiple regression models were developed for each cutting experiments. The aim of the regression models presented in Table 5 is only for extracting the sensitivity information which analyses effect of flank wear propagation on cutting forces and torque.

Cutting forces and torque were used as independent (predictor) variables and maximum flank wear as dependent variable to perform regression models. Table 5 includes the multiple regression models, model correlations and *P*-values for the analyses of the effect of the cutting forces and torque on maximum flank wear.

The multiple regression models are determined by using the Statgraphics [29] statistical analysis software. Results of analyses of variance for the maximum flank wear (V_{Bmax}) regression models supported strong linear relationship (at 95% confidence level) between the variables in the models since model *P*-values less than 0.05 (Table 5). Minimum *P*-values belong to cutting forces (F_x, F_y, F_z) and torque (M_z) are shown in bold In Table 4 which indicate the highest relationship between flank wear. According to distribution intensity of *P*-value results, particularly torque signal M_z but also tangential cutting force F_y and axial force component F_z have significant effect on determination of progressive flank wear.

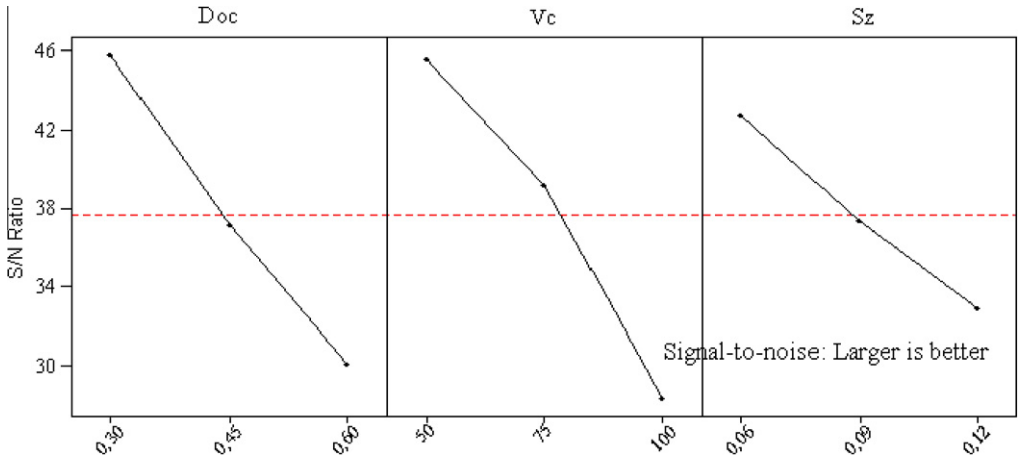

Fig. 5. Main effects plot for tool life with larger is better algorithm.

Table 4
Analysis of variance for tool life.

Source	Sum of squares	Df	Mean square	*F*-ratio	*P*-value
Main effects					
Depth of cut	49573.0	2	24786.5	2.62	0.2763
Cutting speed	48676.8	2	24338.4	2.57	0.2800
Feed per tooth	10476.7	2	5238.37	0.55	0.6437
Residual	18925.4	2	9462.72		
Total (corrected)	127652	8			

4. ANN model for developed TCM system

The actual power and advantage of neural networks lies in their capability to represent both linear and non-linear relationships and in their ability to learn these relationships directly from the data being modeled. Conventional linear models can be insufficient when it comes to modeling data that contains non-linear characteristics. For this reason, an ANN model has been developed for estimating the flank wear of the tool to take the advantage of the neural networks in this study.

4.1. Background

ANN is a mapping method between input and output data based on simulation of biological nervous system, such as the brain, on a computer. It was introduced by McCulloch and coworkers in the early 1940 [30]. Its non-linear mapping architecture produces high flexibility for modeling a system. As a result, ANN has become one of most popular technique used for analyzing the problem without the need to understand its theoretical complexities. This feature of the ANNs is very useful in some circumstance where it is hard to derive a mathematical model. Tool wear considered in this study is very complicated process associated with several parameters. Therefore, ANN is an appropriate technique for developing TCM systems only using experimental samples acquired from metal cutting operations.

An ANN has multilayer architectures consist of massively interconnected processing nodes known as neurons. In the network, each neuron accepts a weighted set of inputs and first forms the sum of the weighted inputs with a bias defined by [31]

$$n = \sum_{i=1}^{P} w_i x_i + b \tag{2}$$

where P and w_i are the number of elements and the weights of the input data x_i. The bias for the neuron is given by b. The knowledge is

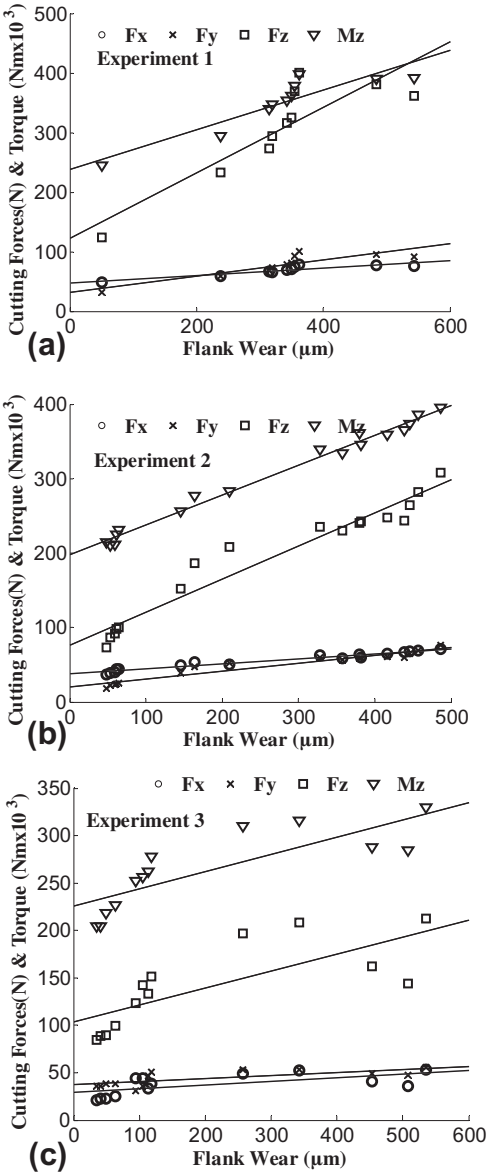

Fig. 6. Cutting forces and torque versus tool flank wear for 0.6 mm depth of cut at different machining conditions.

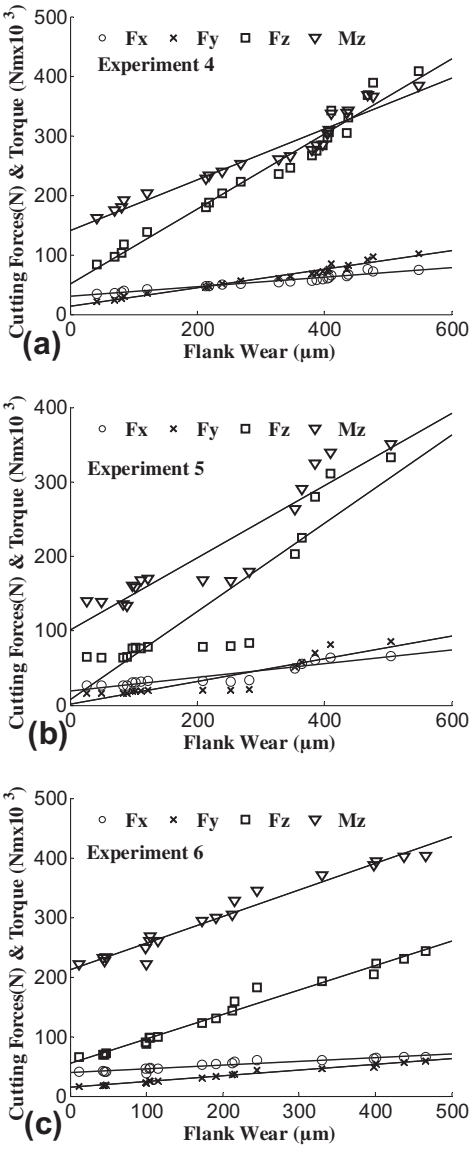

Fig. 7. Cutting forces and torque versus tool flank wear for 0.45 mm depth of cut (Doc) at different machining conditions.

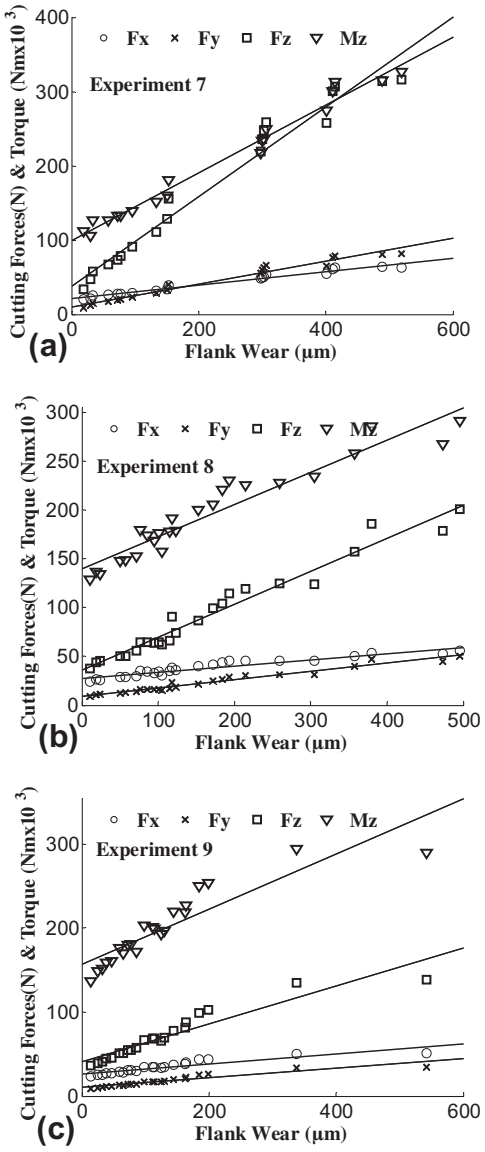

Fig. 8. Cutting forces and torque versus tool flank wear for 0.3 mm depth of cut (Doc) at different machining conditions.

stored in the neuron as a bias and a set of weights. Then, the neuron responds with an output. To this end, the sum of the weighted inputs with a bias is processed through an activation function, represented by f, and the output that it computes is

$$f(n) = f\left(\sum_{i=1}^{P} w_i x_i + b\right) \tag{3}$$

The neuron model emulates the biological neuron that fires when significantly excited, i.e. the neuron's input, n, is large enough. There are many ways to define the activation function such as threshold function, sigmoid function and hyperbolic tangent function.

Using an appropriate learning method, ANNs are trained to perform a particular function by adjusting the values of the connections, i.e. weighting coefficients, between the processing nodes. The training process continues until the network outputs converge to the target. The difference between the network output and the desired output is minimized by modifying the weights and biases. When the difference is below a pre-determined value or the maximum number of approximations is exceeded, the training process is ended. This trained network model can be used to simulate the system outputs for the inputs that have not been introduced before.

The structure of an ANN is usually composed of three parts: an input layer, hidden layers and an output layer. The data contained in the input layer is transformed to the output layer using the hidden layers. Each neuron can receive its input only from the neurons of the lower layer and send its output only to the neurons on the higher layer.

4.2. Implementation of ANN model for tool wear prediction

For development of a TCM system, the total number of 170 wear stages was measured in nine experiments. In order to implement an ANN model, data was divided into two sets namely the training and test sets. For training phase of ANN model, randomly selected 85% of data set was assigned as the training set (145 observations), and the remaining 15% (25 observations) was employed for testing the performance of the network.

The architecture of the ANN for the TCM system, along with its input and output parameters, is illustrated in Fig. 9. The inputs for the

Table 5
Regression models and effects (P) of cutting forces and torque on flank wear (V_{Bmax}).

Experiment no.	$P(F_x)$	$P(F_y)$	$P(F_z)$	$P(M_z)$	Regression model for flank wear (V_B)	$P_{(model)}$	$R_{Squared(\%)}$
1	0.5749	0.094	0.08	**0.0743**	$V_B = -1292.45 - 15.1179 * F_x + 105.757 * F_y - 28.6968 * F_z + 9580.53 * Mz$	0.0063	91.847
2	0.7462	**0.029**	0.0335	0.0418	$V_B = -373.157 + 0.943379 * F_x - 27.7651 * F_y + 7.21062 * F_z + 1719.16 * Mz$	0	99.3067
3	0.0035	0.005	0.0307	**0.0008**	$V_B = -1150.79 - 70.8646 * F_x - 64.1144 * F_y + 12.725 * F_z + 19027.1 * Mz$	0.0003	90.7813
4	0.2788	**0.042**	0.0914	0.2456	$V_B = -125.193 - 7.91111 * F_x + 41.0096 * F_y - 8.82789 * F_z + 1852.34 * Mz$	0	97.6616
5	0.9154	0.907	0.922	**0.7526**	$V_B = -346.037 + 4.90275 * F_x - 3.22894 * F_y - 0.73974 * F_z + 2827.04 * Mz$	0	88.3572
6	0.0022	**0.0006**	0.0157	0.0075	$V_B = -156.781 - 8.12565 * F_x + 25.2045 * F_y - 4.11581 * F_z + 1632.16 * Mz$	0	99.2416
7	0.3069	0.274	0.5322	**0.0906**	$V_B = 27.6786 - 12.4752 * F_x + 19.983 * F_y - 2.85648 * F_z + 1615.35 * Mz$	0	98.2046
8	0.0456	0.0002	**0.0001**	0.0462	$V_B = -19.8345 + 13.6579 * F_x - 207.341 * F_y + 55.767 * F_z - 3269.95 * Mz$	0	98.0291
9	0.3578	0.012	**0.0041**	0.0291	$V_B = 107.942 + 14.0236 * F_x - 241.665 * F_y + 67.7145 * F_z - 4661.52 * Mz$	0	94.0995

ANN model are the cutting conditions, cutting time, RMS values of cutting forces and torque. The output from the ANN is the flank wear. Cutting conditions in the input vector of the ANN model were obtained from the Cutter Location Data (CLDATA) file which was generated by using ProEngineer Wildfire PLM software. The cutting time information was extracted from the difference between the data acquisition start and stop trigger for each cutting pass.

The performance of an ANN is influenced by the characteristics of the network such as the number of hidden layers and the number of nodes in each hidden layer. Since there are no definite methods to determine the optimal number of hidden layers and the neurons on each layer, a significant amount of time during the design of the ANN model is spent on the selection of appropriate variables for network architecture by heuristic search.

The activation (transfer) function in the hidden layer is another important factor influencing the network performance. There are several ways to define the activation function, such as a tangent hyperbolic, logarithmic or a threshold function. For the developed network, a hyperbolic tangent sigmoid function was chosen as activation function in this study as below:

$$f(n) = \frac{e^n - e^{-n}}{e^n + e^{-n}} \tag{4}$$

The input and output data were initially transformed to be in the interval of $[-1, 1]$ using the following equation:

$$p_n = \frac{p - \min(p)}{\max(p) - \min(p)} - 1 \tag{5}$$

where p_n is the transformed form of the data p.

Consequently, by trial and error with different ANN configurations, an optimal, custom designed ANN architecture was found with using MATLAB Neural Network Toolbox. The training data set that is selected randomly, was used to train the network until it gives an approximate function between the input and output parameters. The predictions of the output parameter (V_{Bpre}) were performed using a three layer feed forward ANN with using a back propagation (BP) which is the most popular technique for supervised training of neural networks. BP minimizes an error function, i.e., a mean squared error that is the difference between the actual network output vector and the desired output. An iterative gradient descent technique is used to adjust the weights. The ANN model was trained with four training variations of back propagation methods: Broyden, Fletcher, Goldfarb and Shanno (BFGS) quasi-Newton training method, gradient descent back propagation, and resilient back propagation and Levenberg–Marquardt. Among them, the Levenberg–Marquardt training method provided the best performance; and therefore, was used to adjust the weighting coefficients for ANN model.

As illustrated in Fig. 9 developed ANN model consist of an input layer, a hidden layer and an output layer. The number of neurons in the input and output layers are equal to the number of the input and output parameters, respectively. The hidden layer has 12 neurons for ANN architecture.

Table 6 shows the test data set, which consists of, input parameters of ANN and the actual and predicted output parameter (V_{Bpre}).

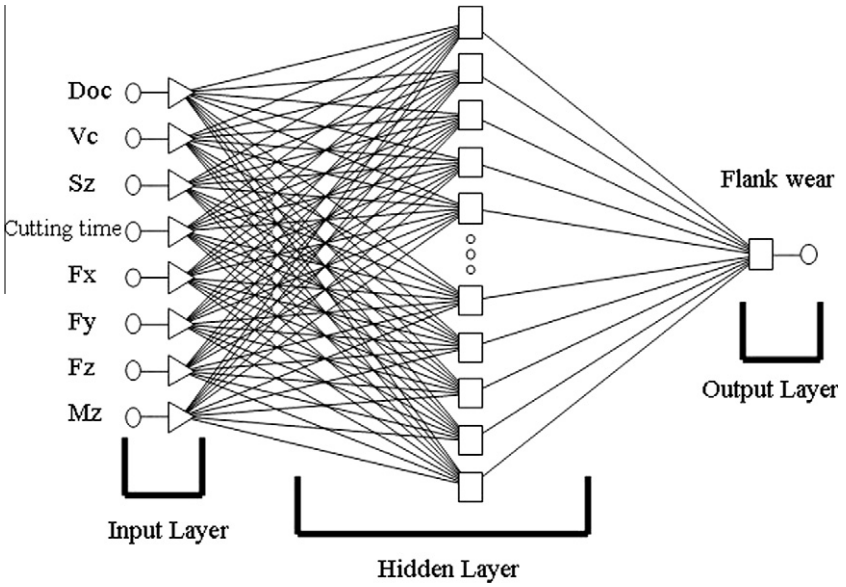

Fig. 9. The structure of ANN for modeling tool condition monitoring system.

4.3. ANN model performance evaluation for TCM system

The performance of the ANN based prediction was assessed by a regression analysis between the network output, i.e. predicted parameters, and the corresponding targets, i.e. experimental values. The criteria used for measuring the network performance are the correlation coefficient, mean relative error and absolute fraction of variance, R^2.

The correlation coefficient assesses the robustness of the relationship between the predicted and experimental results. The coefficient between the actual and predicted outputs is calculated by [32]

$$r(a,p) = \frac{\mathrm{Cov}(a,p)}{\sqrt{\mathrm{Cov}(a,a)\mathrm{Cov}(p,p)}} \tag{6}$$

where $\mathrm{Cov}(a,p)$ is the covariance between the a and p sets that refer to the actual (experimental) output and predicted output sets, respectively, and is defined by [32]

$$\mathrm{Cov}(a,p) = E[(a-\mu_a)-(p-\mu_p)] \tag{7}$$

where E is the expected value, μ_a is the mean value of the set a and μ_p is the mean value of the set p. If the $\mathrm{Cov}(a,p) = 0$, then a and p are expected to be uncorrelated. Similarly, $\mathrm{Cov}(a,a)$ and $\mathrm{Cov}(p,p)$ are the auto covariances of the a and p sets, and are given by

$$\mathrm{Cov}(a,a) = E[(a-\mu_a)^2] \tag{8}$$

$$\mathrm{Cov}(p,p) = E[(a-\mu_p)^2] \tag{9}$$

The correlation coefficient ranges between -1 and $+1$. r Values near to $+1$ indicate a stronger positive linear relationship, while r values near to -1 indicate a stronger negative relationship. The mean relative error, which is the mean ratio between the errors and the experimental values, can be calculated from

$$\mathrm{MRE}(\%) = \frac{1}{N}\sum_{i=1}^{N}\left|100\frac{(a_i-p_i)}{a_i}\right| \tag{10}$$

For the multiple regression analysis a statistical indicator namely the absolute fraction of variance, R^2, can be used

$$R^2 = 1\left(\frac{\sum_{i=1}^{N}(a_i-p_i)^2}{\sum_{i=1}^{N}p_i^2}\right) \tag{11}$$

R^2 ranges between 0 and 1. R^2 value of near 1 shows a very good fit, however near to 0 gives a poor fit.

The predictions of the trained ANN for the performance parameters are given in Fig. 10. The predicted versus target values for the selected 25 flank wear (V_{Bmax}) measurements are shown. Fig. 10 is provided with a straight line indicates a perfect prediction also within an error band of ±10%. This is related to the accuracy of the ANN predictions. As shown in Fig. 10, the ANN predictions for the flank wear yielded a correlation coefficient (r) of 0.992, a mean relative error (MRE) of 5.42% and an absolute fraction of variance (R^2) of 0.996 with the experimental data. These values show that the ANN predicts the flank wear (V_{Bmax}) reliably.

Fig. 10 also shows that, only one predicted flank wear out of randomly selected 25 wear cases remain outside the ±10% error band. As a result, the figure demonstrates a quite satisfactory agreement between the predicted and target values of tool flank wear for developed TCM strategy. The predicted versus observed flank wear values in different experiments for evaluating the ANN performance illustrated in Fig. 11, as well.

5. Conclusion

A neural network based flank wear monitoring system was developed and presented under changing cutting conditions for milling of Inconel 718. ANN model uses cutting conditions, cutting time, buffered real time cutting force and torque data. The network was developed using the data acquired for 170 operations from nine experiments.

According to experimental results, it was observed that torque is an important signal which is not used in most of the TCM system development literature for milling operations. It has been shown from regression equations, M_z signals are most indicative for the flank wear progression than tangential cutting forces (F_x, F_y). The relationship between tool wear propagation and cutting forces-torque variation can also be used for the development of effective tool condition monitoring strategies.

Table 6
The experimental and predicted data obtained under various cutting conditions.

Doc	Vc	Sz	F_x (N)	F_y (N)	F_z (N)	M_z (N m)	Cut. time (min)	V_B (μm)	V_{Bpre} (μm)
0.6	100	0.12	68.97	78.645	315.72	0.35404	2.19	343	331
0.6	100	0.12	75.924	90.929	361.87	0.39128	5.76	543	514
0.6	75	0.09	50.063	52.436	207.88	0.28319	30.24	209	210
0.6	75	0.09	66.561	59.671	244	0.36491	37.55	439	419
0.6	50	0.06	33.617	46.934	133.13	0.26242	88	113	123
0.45	100	0.09	54.042	59.996	235.97	0.25984	9.11	328	307
0.45	100	0.09	54.934	62.457	245.61	0.26599	9.84	346	326
0.45	100	0.09	61.477	76.146	306.13	0.31028	13.12	407	388
0.45	100	0.09	66.029	85.092	342	0.33727	14.21	411	389
0.45	100	0.09	72.445	96.93	388.34	0.36541	20.77	476	498
0.45	75	0.06	30.849	19.548	77.149	0.15856	92.4	103	108
0.45	75	0.06	64.232	81.766	311.37	0.33941	137.13	409	450
0.3	100	0.06	41.76	44.756	175.84	0.19281	99.34	238	189
0.3	100	0.06	49.719	59.921	235.88	0.23384	109.17	300	307
0.3	100	0.06	63.695	80.791	314.67	0.31566	128.82	489	464
0.3	75	0.12	35.232	16.323	64.439	0.1798	31.33	77	84
0.3	75	0.12	32.917	16.027	63.486	0.16854	45.54	95	97
0.3	75	0.12	38.667	23.389	90.874	0.1912	66.67	118	128
0.3	75	0.12	53.585	46.906	185.79	0.28573	118.77	380	412
0.3	75	0.12	55.645	50.542	200.47	0.29096	130.8	495	490
0.3	50	0.09	27.153	11.39	45.048	0.15852	47.67	38	36
0.3	50	0.09	27.203	11.201	44.292	0.16572	68.93	45	44
0.3	50	0.09	33.629	16.748	66.252	0.1929	261.8	125	128
0.3	50	0.09	39.634	22.297	88.274	0.22734	340.27	164	169
0.3	50	0.09	43.338	24.979	99.028	0.2503	368.87	184	186

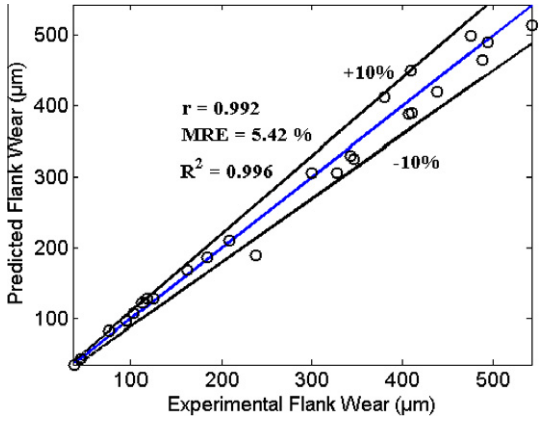

Fig. 10. Experimental (actual) versus predicted wear with correlation factor and mean relative error (MRE). The straight line presents the perfect prediction.

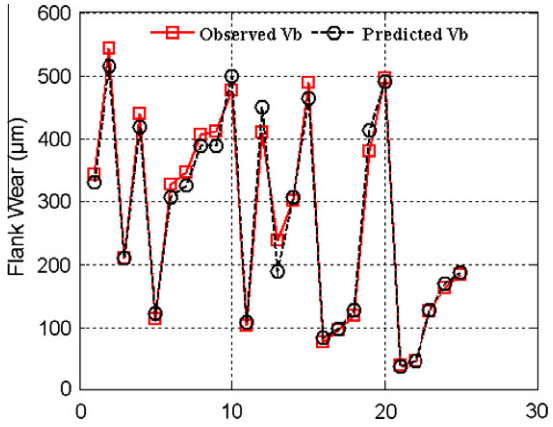

Fig. 11. Experimental (observed) versus predicted values for flank wear.

It was observed that cutting forces and torque signals are both sensitive to cutting conditions. However, during the experiments for some cases the cutting forces and torque reduced with the effect of crater wear development. To model this complicated event and enhance the prediction accuracy for robust tool condition monitoring system a hybrid approach was used by employing cutting conditions and cutting time.

The trained ANN model was tested at 25 different cutting conditions and cutting time intervals. The presented ANN model demonstrated a very good statistical performance with a high correlation of 0.992 between the actual and predicted values for flank wear. The proposed TCM strategy using a rotating cutting force type dynamometer (RCD), can be implemented to complex five axis machining operations e.g. impeller machining.

Acknowledgements

This research was supported by the State Planning Organization (DPT) under the research Grant 2003K120790. The authors thank to Serdar Sevik, and also Fehmi Erzincanli, Mehmet Ermurat, Ilyas Kandemir and Selahattin Uysal for their help and support.

References

[1] Pawade RS, Joshi SS, Brahmankar PK, Rahman M. An investigation of cutting forces and surface damage in high-speed turning of Inconel 718. J Mater Process Technol. doi:10.1016/j.jmatprotec.2007.04.049.
[2] Scheffer C, Heyns Ps. An industrial tool wear monitoring system for interrupted turning. Mech Syst Signal Process 2004;18:1219–42.
[3] Scheffer C, Kratz H, Heyns PS, Klocke F. Development of a tool wear-monitoring system for hard turning. Int J Mach Tools Manuf 2003;43:973–85.
[4] Chungchoo C, Saini D. A computer algorithm for flank and crater wear estimation in CNC turning operations. Int J Mach Tools Manuf 2002;42:1465–77.
[5] Ravindra Hv, Srinivasa YG, Krishnamurthy R. Acoustic emission signals for tool wear identification. Wear 1997;212:78–84.
[6] Zawada Tomkiewicz A. Classifying the wear of turning tools with neural networks. J Mater Process Technol 2001;109:300–4.
[7] Balazinski M, Czogala E, Jemielnaik K, Leski J. Tool condition monitoring using artificial intelligent methods. Eng Appl Artificial Intell 2002;15:73–80.
[8] Ghasempoor A, Jeswiet J, Moore TN. Real-time implementation of on-line tool condition monitoring in turning. Int J Mach Tools Manuf 1999;39:1883–902.
[9] Bahr B, Motavalli S, Arfi T. Sensor fusion for monitoring machine tool conditions. Int J Comput Integr Manuf 1997;10(5):314–23.
[10] Szecsi T. Automatic cutting-tool condition monitoring on CNC lathes. J Mater Process Technol 1998;77:64–9.
[11] Li X. Real-time tool wear condition monitoring in turning. Int J Product Res 2001;39(5):981–92.
[12] Liu Q, Altintas Y. On-line monitoring of flank wear in turning with multilayered feed-forward neural network. Int J Mach Tools Manuf 1999;39:1945–59.
[13] Dimla DE, Lister PM. On-line metal cutting tool condition monitoring I: force and vibration analysis. Int J Mach Tools Manuf 2000;40:739–68.
[14] Dimla DE, Lister PM. Online metal cutting tool condition monitoring II: tool state classification using multi-layer perceptron neural networks. Int J Mach Tools Manuf 2000;40:769–81.
[15] Sharma VS, Sharma SK, Sharma AK. An approach for condition monitoring of a turning tool. In: Proc. ImechE. Part B: J. Engineering Manufacture, vol. 221. doi:10.1243/09544054JEM765.
[16] Chungchoo C, Saini D. On-line tool wear estimation in CNC turning operations using fuzzy neural network model. Int J Mach Tools Manuf 2002;42:29–40.
[17] James LC, Tzeng TC. Multımıllıng-ınsert wear assessment usıng non-linear vırtual sensor, tıme-frequency dıstrıbutıon and neural networks. Mech Syst Signal Process 2000;14(6):945–57.
[18] Ghosh N, Ravi YB, Patra A, Mukhopadhyayc S, Paul S, Mohanty AR, et al. Estimation of tool wear during CNC milling using neural network-based sensor fusion. Mech Syst Signal Process 2007;21:466–79.
[19] Iqbal A, He N, Dar NU, Li L. Comparison of fuzzy expert system based strategies of offline and online estimation of flank wear in hard milling process. Exp Syst Appl 2007;33:61–6.
[20] Tseng PC, Chou A. The intelligent on-line monitoring of end milling. Int J Mach Tools Manuf 2002;42:89–97.
[21] Alauddin M, El-Baradie MA, Hashmi MSJ. End-milling machinability of Inconel 718. Int J Eng Manuf 1996;210:11–23.
[22] Jawaid A, Koksal S, Sharif S. Cutting performance and wear characteristics of PVD coated and uncoated carbide tools in face milling Inconel 718 aerospace alloy. J Mater Process Technol 2001;116:2–9.
[23] Ezugwu EO, Tang SH. Surface abuse when machining cast iron G-17 and nickel-base superalloy (Inconel 718) with ceramic tools. J Mater Process Technol 1995;55:63–9.
[24] Altin A, Nalbant M, Taskesen A. The effects of cutting speed on tool wear and tool life when machining Inconel 718 with ceramic tools. Mater Des 2007;28(9):2518–22.
[25] Nalbant M, Altın A, Gökkaya H. The effect of cutting speed and cutting tool geometry on machinability properties of nickel-base Inconel 718 super alloys. Mater Des 2007;28(4):1334–8.
[26] Alauddin M, El-Baradie MA, Hashmi MSJ. Optimization of surface finish in end milling Inconel 718. J Mater Process Technol 1996;56:54–65.
[27] MATLAB user manual, MathWorks Incorporation; 2006.
[28] Rasband WS, ImageJ US National Institutes of Health, Bethesda, Maryland, USA; 1997–2007. <http://rsb.info.nih.gov/ij/>
[29] STATGRAPHICS centurion version 15 user manual.
[30] Perlovsky LI. Neural networks and intellect. Oxford University Press; 2001.
[31] Haykin S. Neural networks: a comprehensive foundation. New Jersey: McMillan; 1994.
[32] Looney CG. Pattern recognition using neural networks: theory and algorithms for engineers and scientists. New York: Oxford University Press; 1997.